

# Modeling of the interaction between electrons and neutral excited atoms during ELM burst

Junpei INAMORI, Ikuro FUJINO, Akiyoshi HATAYAMA

*Faculty of Science and Technology, Keio University, Yokohama 223-8522, Japan*

(Received: 20 October 2008 / Accepted: 20 January 2009)

The Edge Localized Mode (ELM) burst leads to the serious particle and heat load on the divertor plate. During ELM burst, the electron energy distribution function (EEDF) strongly deviates from Maxwellian. From the viewpoint of the comparison with the spectroscopic measurement, the modeling of the excited atoms is considered to be important. We are developing the numerical program which makes it possible to calculate self-consistently the EEDF and the excited atom density  $n(p)$  during the ELM burst. To check the numerical algorithm, a series of preliminary calculations has been done. The program correctly solves the EEDF and  $n(p)$  in the self consistent manner.

Keywords: Edge Localized Mode (ELM), Boltzmann Equation, Rate Equation, Electron Energy Distribution Function (EEDF), Excited Atom Density

## 1. Introduction

High energy electrons and ions burst into the Scrape-off layer (SOL) from the fusion core plasma during the Edge Localized Mode (ELM). The ELM burst leads to the serious particle and heat load on the divertor plate. Therefore, the modeling and understanding of the effects of the ELM on the SOL/divertor characteristics is one of the most important issues for the divertor design of the future reactors.

Due to the strong deviation from Maxwellian distribution during ELM burst, it is indispensable to develop the kinetic model for analyzing the effect of the ELM burst. The extensive efforts in this direction have been done so far. For example, the particle modelings based on the Particle-in-Cell (PIC) method have been done [1, 2]. In these References, energy relaxation process of ELM particle due to Coulomb collisions, conductive/convective energy transport due to the ELM burst through the SOL/divertor region, the sheath-potential structure during ELM, etc., have been successfully analyzed. Most of these kinetic modelings, however, use a relatively simple model for the interaction between the plasma and neutrals. Quite recently, the PIC-MC (PIC-Monte Carlo) modeling has been done including more detailed model for plasma-neutral interaction. Even in this model, the focus is on the ground state atoms. However, from the viewpoint of the comparison with the spectroscopic measurement, such as the  $H_{\alpha}$  line emission during ELM, the modeling of the excited atoms is considered to be important.

The Collisional Radiative (CR) model is

author's e-mail: inamori@ppl.appi.keio.ac.jp

successfully applied to calculate the population density of the excited atoms for the divertor plasma [3]. The CR model takes into account various atomic processes, such as the electron impact excitation, de-excitation, and radiative decay of the excited atoms. The rate equations including these atomic processes are simultaneously solved to obtain the density of each excited state. The density of each excited state in the steady state can be determined by the balance between the excitation and de-excitation/radiative decay. The CR model plays important roles to interpret the spectroscopic measurement in the experiment and also to evaluate the atomic/molecular density in the experiment.

Most of the conventional CR model, however, is based on the assumption that the energy distribution of the plasma particles involved in the collision processes is in a equilibrium state. In other words, the rate coefficients  $\langle \sigma v \rangle$  used in the rate equations are usually calculated from Maxwellian distribution in most of the conventional CR modelings of SOL/divertor plasmas. As mentioned above, the velocity distribution in the SOL/divertor region during the ELM strongly deviates from Maxwellian.

The purpose of this study is to develop the numerical program which makes it possible to calculate self-consistently the electron energy distribution function (EEDF) and the excited atom density during the ELM burst. In the program, the Boltzmann equation for the electrons and the rate equation for the excited atoms are numerically solved. The brief summary of the program and several test/preliminary calculations for the analysis

of the ELM burst will be presented.

## 2. Basic Equation and Numerical Model

### Basic equation for electrons

In order to solve the Boltzmann equation for the electrons, trajectories of the test electrons are directly followed in the phase space by their equation of motion:

$$\frac{d\mathbf{v}}{dt} = -\frac{e}{m_e}(\mathbf{E} + \mathbf{v} \times \mathbf{B}) + \left(\frac{d\mathbf{v}}{dt}\right)_{\text{collision}} \quad (1)$$

where  $m_e$ ,  $e$ ,  $\mathbf{E}$  and  $\mathbf{B}$  are the mass, elementary charge, electric field and magnetic flux density, respectively. The last term on the right hand side (RHS) in Eq. (1) denotes the velocity change due to the collisions.

In the numerical time-integration of Eq. (1), we have used the principle of separation [4]. That is, the first term (particle motion) and the second term (collision term) of the RHS in Eq. (1) can be treated separately, if the time step  $\Delta t$  is sufficiently small. The leap frog method [5] is applied to the time integration of the first term on the RHS of Eq. (1). On the other hand, the velocity change due to the collisions is taken into account by Monte Carlo techniques at each time-step as follows.

Collision processes are classified into mainly two categories; inelastic collisions with neutrals and elastic collision with electrons (e-e Coulomb collision). As for the inelastic collision process, such as ionization, excitation and de-excitation, the null-collision method is applied [4]. The method and procedure are briefly summarized as follows. (1) First, prior to the electron test flight, the free-flight time  $t_{\text{free}}$  is calculated from the initial energy of each test electron and the total cross section of inelastic collisions taken into account in the analysis. (2) Next, at each time step along their trajectory, whether the collision occurs or not is judged from the comparison of the flight time  $t_f$  with the free flight time  $t_{\text{free}}$ . (3) When collision occurs, the kind of the inelastic collision is determined by the ratio of mean free path of each collision kind to the total mean free path. (4) Finally, the velocity and the energy change due to the inelastic collision are calculated in the same manner as shown in Ref. [6]. Then, the above procedure from (1) to (4) is repeated until the test electron reaches the calculation boundary or is lost due to recombination. In addition, in case of ionization collision, trajectory of the secondary electron is followed from their birth point by the same procedure.

Coulomb collisions are taken into account in the present study by the Binary Collision Model (BCM) in Ref. [7]. The basic procedure of this method is summarized as follows. (1) First, a pair of electrons is randomly chosen from the system and their relative velocity  $\mathbf{u} = \mathbf{v}_i - \mathbf{v}_j$  is calculated. (2) Next, the scattering angles,  $\chi$  and  $\Phi$ , are determined in the

following way: the angle  $\chi$  is randomly selected from the Gaussian distribution with its mean  $\langle \delta \rangle = 0$  and the variance

$$\langle \delta^2 \rangle = n_e e^4 \ln \Delta t / (8\pi \epsilon^2 m_e u^3) \quad (2)$$

where  $\delta \equiv \tan(\chi/2)$ ,  $\Delta t$  is the time step and the remaining notations are the conventional ones. On the other hand, the angle  $\Phi$  is chosen by  $\Phi = 2\pi U$ , where  $U$  is a uniform random number. (3) From these scattering angles, the relative velocity change  $\Delta \mathbf{u}$  due to Coulomb collision is calculated. (4) Finally, the velocity changes of each electron involved in the collision event  $\Delta \mathbf{v}_i$  and  $\Delta \mathbf{v}_j$  are obtained from  $\Delta \mathbf{u}$ .

### Basic equation for neutral atoms

The population density of the excited atoms is calculated from the following system of the rate equations:

$$\begin{aligned} \frac{dn(p)}{dt} = & \left[ \left\{ \sum_{q < p} C(q, p) + \sum_{q > p} F(q, p) \right\} n_e + \sum_{q > p} A(q, p) \right] n(q) \\ & - \left[ \left\{ \sum_{q > p} C(p, q) + \sum_{q < p} F(p, q) \right\} n_e + S(p) n_e + \sum_{q < p} A(p, q) \right] n(p) \\ & + \{ \alpha(p) n_e + \beta(p) \} n_e H^+ \end{aligned} \quad (3)$$

where  $n(p)$  and  $n(q)$  are the density of the excited atom with the principal quantum number  $p$  and  $q$ . The rate coefficients of the electron impact excitation and de-excitation are denoted by the symbol  $C(p, q)$  and  $F(p, q)$ . In addition,  $A(p, q)$  is the spontaneous transition probability from  $p$  to  $q$ ,  $S(p)$  is ionization coefficient for  $p$ ,  $\alpha(p)$  is the three-body recombination rate coefficient for  $p$ , and  $\beta(p)$  is the radiative recombination rate coefficient for  $p$ .

The numerical program is being developed to solve Eq. (1) and Eq. (3) based on the numerical method described above. The numerical program mainly consists of two modules: (1) Electron module (EM-module), which solves Eq. (1) to obtain the electron velocity distribution function  $f_e(\mathbf{v})$ , and (2) Neutral atom module (NAM-module) to solve Eq. (3) and obtain the population of the excited atoms  $n(p)$ . In order to obtain self-consistent solutions of  $f_e(\mathbf{v})$  and  $n(p)$ , two modules have to be coupled together. The coupling scheme and input/output parameters for each module are summarized in Fig. 1. From the electron velocity distribution calculated from the EM-module, the electron density and the rate coefficients are calculated. For example, the rate coefficient of the electron impact excitation from the  $p$  to  $q$  state  $C(p, q)$  is calculated by

$$\begin{aligned} C(p, q) = & \frac{1}{n_e} \int \sigma_{p \rightarrow q}(\mathbf{v}) \mathbf{v} f_e(\mathbf{v}) d^3 \mathbf{v} \\ n_e = & \int f_e(\mathbf{v}) d^3 \mathbf{v} \end{aligned} \quad (4)$$

where the cross section  $\sigma(\mathbf{v})$  is estimated from the analytic formula [8-10]. From these rate coefficients, the

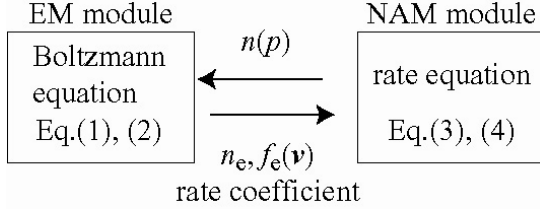


Fig. 1 EM module and NAM module

NAM-module outputs each population density  $n(p)$  of the excited neutral atoms, which in turn is used to estimate mean collision time (such as  $t_{\text{coll}} = n(p)\sigma(\mathbf{v})\mathbf{v}$ ) of the electron impact excitation, de-excitation and ionization in the EM-module.

### 3. Preliminary calculations

#### Test calculation for the EM module

In order to validate the EM-module, the module has been applied to the analysis of the EEDF in the multi cusp arc-discharge plasma [11], where the experimental estimate of the EEDF is available.

The simulation code developed here has three key features. First, collisions between electrons are taken into account. Second, some inelastic collisions between electrons and neutral particles are taken into account. The inelastic collisions which are taken into account in this test calculation are summarized in Table 1. Third, realistic geometry and magnetic field configuration are taken into account in our three-dimensional code.

Time step of calculation is  $\Delta t = 10^{-8}$  s which is much smaller than the Larmor period of the electrons in the source. Every  $10^{-8}$  s, Coulomb collision is taken into account and the inelastic collision events are judged to occur or not. The dimension of the plasma chamber is as follows:  $-120 < x < 120$  mm,  $-240 < y < 240$  mm, and  $0 < z < 203$  mm. The sheath potential drop at the wall is kept at 3V.

There are sixty-six magnets installed around the surfaces of the source that work as cusp magnets or filtering magnets for electron confinement. The number

Table 1 Reaction taken into account in the simulation code (Ref. 12)

Index	Collision species	Before	After
a	Excitation	$e + \text{H}(1s)$	$e + \text{H}^*(2p)$
b	Ionization	$e_1 + \text{H}(1s)$	$e_1 + e_2 + \text{H}^+$
c	Vibrational excitation	$e + \text{H}_2(v=0)$	$e + \text{H}_2(v=1)$
d	Electronic excitation	$e + \text{H}_2(X^1\Sigma_g^+)$	$e + \text{H}_2(B^1\Sigma_u^+ 2p\sigma)$
e	Electronic excitation	$e + \text{H}_2(X^1\Sigma_g^+)$	$e + \text{H}_2^*(b^3\Sigma_g^-)$ $e + \text{H}_2^*(a^3\Sigma_g^+)$ $e + \text{H}_2^*(c^3\Pi_u^-)$
f	Dissociation	$e + \text{H}_2(X^1\Sigma_g^+)$	$e + \text{H}(1s) + \text{H}^*(2s)$
g	Ionization	$e + \text{H}_2(X^1\Sigma_g^+)$	$e + \text{H}_2^+(v) + e$
h	Dissociative recombination	$e + \text{H}_2^+(0 \ll v \ll 9)$	$\text{H}(1s) + \text{H}^*(n \gg 2)$
i	Dissociative recombination	$e + \text{H}_3^+$	$\text{H} + \text{H} + \text{H}$

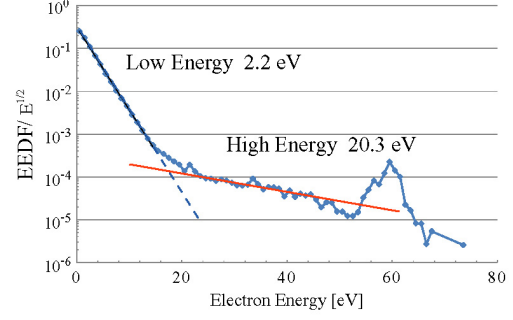


Fig. 2 Electron energy distribution

of magnets placed on each surface is as follows: six on the front plate; eight on the bottom; six on the back plate; four on each surface of the two sidewalls; four on the sides for filter region; and thirty on the extraction region. The magnetic field configuration in the above condition is calculated by using the three-dimensional analytical solution based on the magnetic charge model.

We set several parameters of the source. First, pressure is set as  $p = 0.3$  Pa. Second, throughout the simulation, temperature of  $\text{H}_2$  molecule is maintained to be 300K and dissociation rate of  $\text{H}_2$  molecule is 10%. Third, arc voltage of the filament is 60V and arc current is 166.7A (arc power is 10kW). Fourth, densities of ionized hydrogen particles are  $\text{H}^+ = 3.0 \times 10^{17} \text{ m}^{-3}$ ,  $\text{H}_2^+ = 6.0 \times 10^{17} \text{ m}^{-3}$ , and  $\text{H}_3^+ = 1.0 \times 10^{17} \text{ m}^{-3}$ . Note that the densities of neutral and ionized hydrogen particles are kept constant for simplicity. Every  $10^{-8}$  s, 100 test electrons are emitted isotropically from the filaments. For simplicity, we suppose that electrons are accelerated to 60eV instantaneously in the plasma sheath around the filament. That is, the incident energy of the electrons is taken as 60V.

The calculation was continued until the electron density becomes steady state. The calculated EEDF is shown in Fig. 2. There are two energy populations in the numerical result and this tendency is consistent with an experimental result [13, 14]. In this calculation, two temperature populations are obtained as approximately 2.2 and 20.3eV. This tendency and temperature reasonably agree with those in the experiments under almost the same experimental conditions in the JAEA 10 ampere source [13, 14].

#### Test calculation for the NAM module

In order to validate the NAM-module, the module has been applied to the analysis of the excited atomic density  $n(p)$ .

In Ref. [3], Sawada have solved the rate equations Eq. (3) with  $T_e = 10$  eV (Maxwellian distribution),  $n_e = 10^{18} \text{ m}^{-3}$  and  $n(1) = 10^6 \text{ m}^{-3}$ . With the given EEDF under the same condition as in Ref. [3], the rate coefficients  $C(p, q)$  and  $S(p)$  are calculated from Eq. (4)

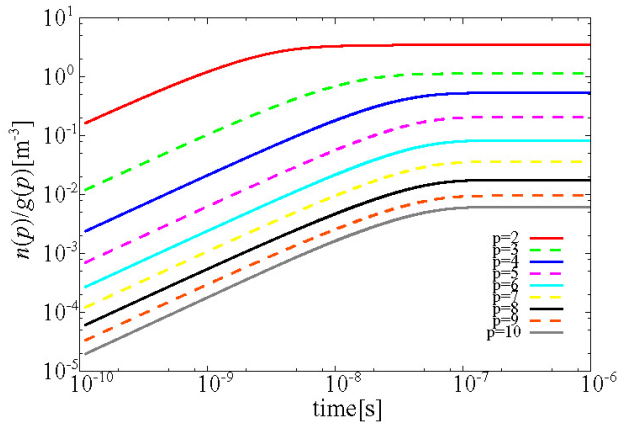


Fig. 3 Time evolution of the density of the excited atoms

and the NAM module starts calculating the excited atomic density  $n(p)$  from Eq. (3) with the time step  $\Delta t = 10^{-11}$  s. Figure 3 shows the results for the time evolution of  $n(p)$ . Our numerical results of  $n(p)$  in Fig. 3 agree well those by Sawada, not only for the steady state, but also for the time evolutions.

From above test calculations and comparisons with the results by Sawada, it is confirmed that the numerical algorithm correctly works to calculate the rate coefficients from Eq. (4) with the given EEDF. It is also validated that the numerical time-integration of the rate equation in the NAM module gives correct result.

#### Preliminary coupling of the EM and NAM module

After the independent check of the EM and the NAM module, these are coupled together in order to obtain self consistent solutions of  $f_e(v)$  and  $n(p)$ . Preliminary calculations have been done to check the program using the relatively simple 1D geometry shown in Fig. 4.

The system length in the  $x$ -direction is taken to be  $L = 2$  m, while the system has infinite lengths in the  $y$  and  $z$  direction.

For the purpose of the preliminary calculations, we set several conditions and parameters. First, we set  $\mathbf{E} = \mathbf{B} = 0$  in Eq. (1). Second, neutral atom pressure and temperature are set as  $p_0 = 1.33$  Pa,  $T_H = 500$  K, respectively. Third, the principle quantum number  $p$  is taken into account from  $p = 1$  to  $p = 10$ . And the initial density of excited atomic  $n(p)$  is zero while the initial ground state density  $n(1)$  is set as  $n(1) = p_0 / kT_H$ . Fourth, the inelastic collisions which are taken into account in the EM-module are summarized in Table 2. The three-body recombination and the radiative recombination processes are neglected. Fifth, incident test electron energy is set to be 10eV or 100eV as in Fig. 5 (a).

Test electrons are injected from the left boundary at the constant rate (one particle per  $\Delta t = 10^{-8}$  s). The test electrons reaching the right boundary  $x = L$  are either absorbed or reflected depending on the electron energy. If

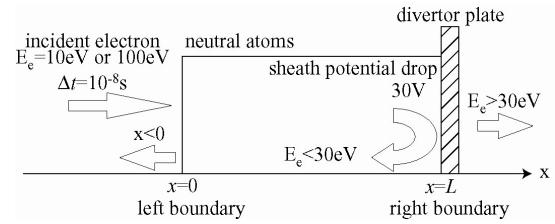


Fig. 4 Test geometry

the test electron energy is lower than sheath potential drop, 30V, then test electrons are reflected by changing the sign of the velocity component  $v_x$  in the  $x$  direction. On the other hand, test electrons which have higher energy than sheath potential energy and those reaching the left boundary  $x = 0$  are absorbed. In this manner, the total number of test electrons in the region in Fig. 4 starts increasing and finally it reaches a steady state.

With the EEDF obtained by the EM module, the rate coefficients  $C(p, q)$ ,  $F(p, q)$  and  $S(p)$  are calculated from Eq. (4) every  $10^{-8}$  s and the NAM module starts calculating the excited atomic density  $n(p)$  from Eq. (3) with the rate coefficients above and  $A(p, q)$  with the time step  $\Delta t = 10^{-11}$  s.

In these preliminary calculations, we assume relatively simple model for the time evolution of incident electron energy. We first set incident electron energy to be 10eV. Then after obtaining the steady state with lower electron energy, we suddenly change the incident electron energy to 100eV for a period 0.1ms to simulate the ELM burst as shown in Fig. 5 (a). Time evolution of electron density  $n_e$ , average electron energy, and density of the excited atom  $n(3)$  with  $p=3$  are shown in Fig. 5 (b), (c), and (d), respectively.

In Fig. 5 phase 2, electron density begins to increase. Also, average electrons energy increased rapidly and then decreases gradually. And time evolution of  $n(3)$  seems to follow that of incident electron energy. Since incident electron energy is set to be 100eV in this phase, the number of electrons that have greater energy than the threshold energy of excitations and ionizations would increase. As a result, there are more excitation and ionization events. Thus, the electron density starts increasing due to the increasing number of secondary electrons by ionization. At the same time, average electron energy, which was once rapidly increased by the high electron energy pulse, might begin to decrease gradually since incident electron energy is lost by

Table 2 Reaction taken into account in the simulation

Index	Collision species	Before	After
a	Excitation	$e + n(p)$	$e + n(q)$
b	De-excitation	$e + n(q)$	$e + n(p)$
c	Ionization	$e_1 + n(p)$	$e_1 + e_2 + H^+$

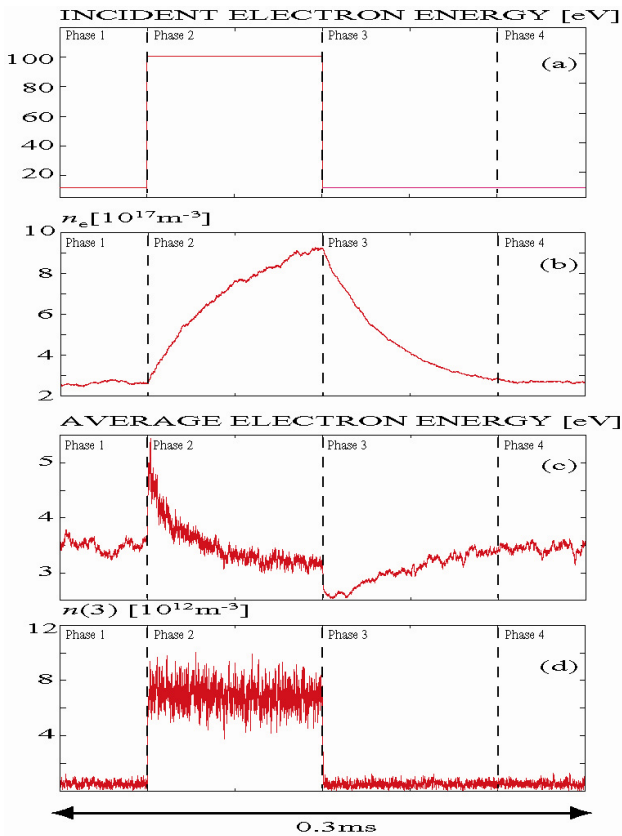


Fig. 5 Incident electron energy is shown in (a), and time evolution of electron density, average electron energy, and  $n(3)$  are shown in (b), (c), and (d), respectively

collisions with atoms.

In Fig. 5 phase 3, the incident energy is set to be 10eV again. In contrast of the phase 2, collisions with atoms would decrease since the number of electrons which have more energy than threshold energy would decrease. As a result, electron density decreases, because the effect of electron-loss at the divertor plate or at  $x=0$  dominates the production of secondary electrons by ionization. Also, the total electron energy decreases due to the change of the incident energy in phase 3. On the other hand, the number of the electrons gradually decreases. Thus, the number of the electrons in phase 3 is larger than that in the steady state and saturated. As a result, the average electron energy decreases rapidly and is lower than that in the phase 1.

These preliminary results show that the EM module and the NAM module are successfully coupled in the program. Although the program is still under the development, it is verified that the program is useful to analyze time evolution of the EEDF and  $n(p)$ .

#### 4. Summary

We develop the numerical code which can calculate self-consistently the electron energy distribution function

and the excited atom density. The code consists of the EM module and the NAM module. In order to validate the EM module, the module has been applied in the multi cusp arc-discharge plasma. The NAM module has been verified by comparing its result with Ref. [3]. Those two modules are coupled. The preliminary results show that program correctly calculates the electron energy distribution function and neutral excited atom density for simple cases. Although the program is still under the development phase, the program has a potential to be a useful tool for the analysis of the EEDF and excited atom population and for the comparison with spectroscopic measurement, such as the  $H_\alpha$  line emission during ELM.

For further development, the ion dynamics should be included. Also, the full PIC technique which can include self-consistent electron field during ELM should be applied to the code.

#### Acknowledgement

This study is partially supported by a Grant-in-Aid for Scientific Research of the Japan Society for the Promotion of Science

- [1] T. Takizuka and M. Hosokawa, *Contrib. Plasma Phys.*, **46**, 698 (2006)
- [2] A. Bergmann, *Nucl. Fusion* **42**, 1162 (2002)
- [3] K. Sawada, Ph. D. thesis, Kyoto University (1994)
- [4] K. Nanbu, *IEEE Trans. Plasma Sci.* **28**, 971 (2000)
- [5] C. K. Birdsall and A. B. Langdon, *Plasma Physics via Computer Simulation* (McGraw-Hill, New York, 1985)
- [6] K. Matyash, “Kinetic modeling of multi-component edge plasmas”, Ph. D. thesis, Ernst-Moritz-Armdt-Universitat, Greifswald, 2003
- [7] T. Takizuka and H. Abe, *J. Comput. Phys.* **25**, 205 (1977)
- [8] L. C. Johnson, *Astrophys. J.* **174**, 227 (1972)
- [9] L. Vriens and A. H. M. Smeets, *Phys. Rev. A* **22**, 940 (1980)
- [10] K. Sawada, K. Eriguchi, and T. Fujimoto, *J. Appl. Phys.* **73**, 8122 (1993)
- [11] I. Fujino, A. Hatayama, and N. Takado, *Rev. Sci. Instrum.* **79**, 02A510 (2008)
- [12] R. K. Janev, W. D. Langer, K. Evans, Jr., and D. E. Post, Jr., *Elementary Processes in Hydrogen-Helium Plasma, Cross Sections and Reaction Rate Coefficients* (Springer, Berlin, 1987)
- [13] N. Takado, J. Hanatani, T. Mizuno, A. Hatayama, H. Tobar, M. Hanada, T. Inoue, M. Taniguchi, M. Dairaku, M. Kashiwagi, K. Watanabe, and K. Sakamoto, *AIP Conf. Proc.* **925**, 38 (2007)
- [14] M. Hanada, T. Seki, N. Takado, T. Inoue, H. Tobar, T. Mizuno, A. Hatayama, M. Dairaku, M. Kashiwagi, K. Sakamoto, M. Taniguchi, and K. Watanabe, *Rev. Sci. Instrum.* **77**, 03A515 (2006)